Tellus
SERIES B
CHEMICAL
AND PHYSICAL
METEOROLOGY
PUBLISHED BY THE INTERNATIONAL METEOROLOGICAL INSTITUTE IN STOCKHOLM

Tellus (2009), 61B, 669–676
Printed in Singapore. All rights reserved

TELLUS

Differentiating natural and anthropogenic cloud condensation nuclei in the California coastal zone

By D. A. HEGG[1]*, D. S. COVERT[1], H. H. JONSSON[2] and R. WOODS[2], [1]*Department of Atmospheric Sciences, University of Washington, Seattle, WA, USA;* [2]*Meteorology Department, Naval Post Graduate School, Monterey, CA, USA*

(Manuscript received 20 February 2009; in final form 15 June 2009)

ABSTRACT

Aerosol samples were collected and cloud condensation nuclei (CCN) concentrations at five supersaturations were measured along and off the central California coast within the cloud-topped, marine boundary layer from aircraft flights during August 2007. Receptor modelling has been applied to estimate the natural versus anthropogenic source contribution of cloud condensation nuclei in this region, a region of climatically important marine stratocumulus. The results suggest that anthropogenic CCN accounted for about 50% of the CCN active at 0.3% supersaturation in this region during the measurement period.

1. Introduction

The significant impact of anthropogenic aerosols on the albedo of shallow layer clouds, particularly in the marine environment, is now well established (e.g. Platnick and Twomey, 1994; Durkee et al., 2000; IPCC, 2001). However, it has proven to be difficult to quantitatively associate anthropogenic aerosol concentrations active as cloud condensation nuclei (CCN) with specific cloud albedos (cf. Avey et al., 2007). One link in the chain that has proven particularly elusive is the necessary differentiation of anthropogenic CCN from natural in the areas of impact. For the extreme case of ship tracks, in which the aerosol interacting with clouds has been overwhelmingly anthropogenic, a good deal of fruitful work has been done, though even here the background concentration of marine aerosol appears to modulate the impact of the anthropogenic aerosol, rendering a pure anthropogenic signal difficult to obtain (e.g. Platnick et al., 2000). Furthermore, while an important limiting case for assessment of impact, ship tracks are of little moment in determining the overall climatic impact of anthropogenic aerosols on marine stratocumulus decks. For more representative conditions in the marine atmosphere, anthropogenic and natural CCN are difficult to distinguish, in large part because they both tend to be internal mixtures of compounds many of which have both natural and anthropogenic sources.

Several strategies have been used to address this issue, with mixed results. For example, Novakov and Penner (1993), and later Rivera-Carpio et al. (1996) used size resolved impactor data to obtain the mass distribution of various chemical species, converting them to aerosol number distributions, and then compared the cumulative number distributions with simultaneously measured CCN activation spectra to determine the fraction of CCN number attributable to the measured chemical species. The approach requires that the chemical composition as a function of size be well known and highly size-resolved over the CCN size range. This condition is seldom met or even evaluated. The utility of this approach also depends greatly on the aerosol mixing state, leading to unambiguous results only for the extreme case of complete external mixing—which is rare (e.g. Murphy et al., 2006; Phinney et al., 2006). It does not, furthermore, address the point that a number of chemical species commonly found in CCN have both anthropogenic and natural sources (e.g. sulphate). Similarly, assessments of CCN composition based on the thermal volatility of the particles have proven enlightening, revealing the importance of various organic and inorganic species, but cannot really be said to differentiate anthropogenic and natural CCN (e.g. Ishizaka and Adhikari, 2003). Even the most recent and technologically sophisticated studies, involving simultaneous individual particle chemical analysis and CCN activity measurements cannot completely resolve the issue of source attribution based on composition alone. Indeed, they highlight another difficulty of such attribution, namely, the significant modification of the composition and CCN activity brought about by in situ chemistry (e.g. Furutani et al., 2008).

*Corresponding author.
e-mail: deanhegg@atmos.washington.edu
DOI: 10.1111/j.1600-0889.2009.00435.x

Table 1. Species analysed from the filter samples obtained in the study. Technique acronyms are defined in the text. Mean and standard deviation of the concentrations found during the study are given (μg m^{-3})

Species	Technique	Mean	*SD*	Used in UNMIX
Acetate	IC	0.19	0.32	No
Formate	IC	0.04	0.06	No
Chloride	IC	1.28	1.5	Yes
Nitrate	IC	0.56	0.58	Yes
Glutarate	IC	0.01	0.07	No
Succinate	IC	0.01	0.05	No
Sulphate	IC	1.25	0.65	Yes
Oxalate	IC	0.09	0.19	Yes
Boron	ICP-OES	0.05	0.18	No
Calcium	ICP-OES	0.03	0.08	No
Iron	ICP-OES	0.0001	0.0002	No
Potassium	ICP-OES	0.14	0.13	No
Magnesium	ICP-OES	0.04	0.07	Yes
Sodium	ICP-OES	0.81	0.82	Yes
Silicon	ICP-OES	0.12	0.04	No
Lead	ICP-OES	0.47	0.80	Yes
Phosphate	ICP-OES	0.54	1.1	No
Total dry mass	Gravimetric	16.3	16.6	Yes
NSS Potassium	Derived	0.11	0.11	Yes
NSS Sulphate	Derived	1.04	0.58	Yes
Soluble mass	IC/ICP	5.3	3.4	Yes
Black carbon	Absorption photometer	0.26	0.82	Yes
Sub-H_2O[a]	AHS	22.3	21.3	Yes
Super-H_2O[b]	AHS	7.1	6.1	Yes
Scat-H_2O[c]	Humidigraph	6.5	4.2	Yes

[a]Water of hydration of the submicron aerosol (from AHS).
[b]Water of hydration for the supermicron aerosol (from AHS).
[c]Water of hydration from the humidigraph.

To address the general problem of aerosol source attribution, various analyses of variance techniques (ANOVA) have long been employed (e.g. Cheng et al., 1993; Song et al., 1999; Kim et al., 2004; Chen et al., 2007). Such techniques, sometimes termed receptor modelling, have proven very versatile and useful in source attribution of aerosol mass and size distribution. We adopt this approach here for CCN source attribution in the marine environment, using the results to distinguish anthropogenic and natural CCN.

2. Methodology

To characterize the chemical composition of the aerosol, filter sampling was employed. Normally, 47 mm Teflo membrane filters with a 2 μm pore size were used. On a few occasions, sufficient sampling time was available to collect size-resolved filter samples via five stage Micro Orifice Impactors (MOI) followed by a filter backup. The substrates for this type of sampling were Zefluor Teflon filters (1 μm pore size). Both substrates have collection efficiencies in excess of 99.99% for 0.2 μm particles and larger. After collection, samples were stored at a nominal 4°C prior to analysis. The samples were analysed over a week's time. All substrates were analysed gravimetrically and then extracted in 10 ml of HPLC water. The extracts were then analysed by standard Ion Chromatography (IC) for anions (both organic and inorganic), Liquid Chromatography–Mass Spectroscopy (LC–MS) for carbohydrates and Inductively Coupled Plasma–Optical Emission spectroscopy (ICP-OES) for a suite of trace elements (cf. Gao et al., 2003b). The suite of species analysed is given in Table 1 together with the mean and standard deviation of the concentrations found during the study. The hygroscopic properties of the aerosol were determined by measuring the light scattering coefficient at three relative humidities, nominally 40, ambient and 85% (Gasso et al., 2000), and by use of an Aerosol Hydration Spectrometer (Hegg et al., 2008). Additionally, in order to quantify the concentration of light absorbing carbon present (important both optically and as an aerosol source tracer), we used a three wavelength Particle Soot Absorption Photometer (PSAP) to measure the aerosol absorption coefficient (Virkkula et al., 2005). We then employed a specific black carbon absorption coefficient of 7 m^{2}g^{-1} to convert the absorption at 530 nm to light absorbing carbon mass concentration (cf. Bond and Bergstrom, 2006).

The other main measurement in this study is that of the CCN activation spectrum. For this, we use the DMT Inc. CNN-100 CCN spectrometer that employs the design described by Roberts and Nenes (2005). It measured cumulative CCN number concentrations at nominal supersaturations of 0.2, 0.3, 0.5, 0.7 and 1.0%.

The instruments described above were deployed from an airborne platform, the Center for Interdisciplinary Remotely Piloted Aircraft Studies (CIRPAS) Twin Otter research aircraft. This platform, and its associated facility instruments, has been described in a number of publications (e.g. Wang et al., 2002; Schmid et al., 2003; Hegg et al., 2005). More specific information on the measurements will be related, as necessary, in the discussion.

The aerosol chemical composition can, in some instances, be used to evaluate possible aerosol sources. However, unless the sources are well characterized with respect to composition and size-distribution, and differ significantly from one another, fully deterministic assessment, using tools such as a chemical mass balance model, is not really feasible since even the relative species emissions are not known and mass conservation cannot be assessed. Such is the case here and to address the issue of sources of CCN active aerosol, we have employed alternative ANOVA techniques. Specifically, we have used, in addition to the standard factor analysis with principal component extraction (cf. Gao et al., 2003a), the EPA PMF 1.1 and UNMIX 2.3 models. These are operational, regulatory, receptor models used precisely

to deconvolute aerosol sources when good source profiles are not available. Numerous examples of their application to such issues are in the literature (e.g. Willis et al., 2001; Kim et al., 2004).

3. Venue

The measurements reported here were acquired during the Cloud-Aerosol Research in the Marine Atmosphere IV (CARMA-IV) field campaign. The CARMA Project has been an ongoing effort to elucidate both the direct and indirect effects of aerosols on marine boundary layer (MBL) structure and the radiative balance of the marine atmosphere. Our current specific goals (as per the above discussion) thus fit comfortably into the CARMA framework.

The venue for the CARMA measurements is the California coastal zone, extending from 37.2°N Latitude to 34°N latitude and from the coastline to ∼300 km offshore. This location is well suited to the study goals for a number of reasons. It is one of the three most intensive stratocumulus areas in the world (Warren et al., 1988) and the clouds have been shown susceptible to both microphysical and radiative perturbation by aerosols (cf. Platnick and Twomey, 1994; Durkee et al., 2000, and references therein). Most relevant to the present study, it is also an area in which the aerosol is impacted by a number of different sources, including biomass burning, pollution and the ocean surface (Hegg et al., 2008). This leads to a wide range in both aerosol size and composition, and other derivative properties such as the CCN activity (cf. Roberts et al., 2006). Airborne sampling was done throughout this region in the course of 15 flights conducted during August 2007. Horizontal traverses of the MBL were made. There were normally at least three per flight, typically at 30 m MSL and also 100–500m but below cloud base (when cloud was present). From this set, 24 traverses had sufficiently complete chemical data to permit inclusion in receptor modelling analysis (Hegg et al., 2008). Of these, 16 had sufficiently good CCN data to warrant co-analysis of the chemistry and CCN activity. The criterion for selection of the CCN spectra was two-fold. First, measurements for at least three supersaturations (in 14 of the 16 cases it was 4 or more) had to be available over the filter-sampling interval from which the chemical data were derived. Second, the total particle number concentration during the sampling interval had to be relatively constant (within ±15%) to ensure that the concentrations at the various supersaturations were comparable. The samples with good CCN data are all given in Table 2.

Table 2. Values of total particle concentration and mass for each of the samples for which good CCN spectra were available

Sample no.	Date	Time (UTC)	Total particle concentration (cm^{-3})	Total mass concentration ($\mu g\ m^{-3}$)
1	11 August	1811	701	5.4
2	11 August	1845	662	9.7
3	13 August	1919	4877	11.4
4	13 August	1956	6104	56.3
5	14 August	1841	2703	13.9
8	15 August	1753	583	7.8
9	17 August	1945	1011	5.2
10	21 August	1828	480	4.3
11	21 August	1900	197	5.5
14	22 August	1920	957	20.7
15	22 August	1958	951	16.0
16	24 August	1930	2037	17.5
17	25 August	1904	369	6.0
19	26 August	1805	431	7.7
22	27 August	1745	930	15.4
23	27 August	1845	953	16.5

4. Results and discussion

4.1. Chemistry and aerosol sources from receptor modelling

The available data set consists of the concentrations of 25 chemical species analysed in each of 24 filter samples measured concurrently with two measures of aerosol hygroscopicity. From these, several derivative variables such as non-sea salt (NSS) sulphate and potassium, and water of hydration were calculated (Hegg et al., 2008). On the other hand, several species were eliminated from use a priori due to a low incidence of above detection limit concentrations—which led to a poor signal-to-noise ratio (see Table 1 for the species used in the UNMIX analysis). Unfortunately, one such set of species was the carbohydrates, including levoglucosan. This species has been widely used as an excellent biomass burning tracer (cf. Simoneit et al., 1999; Gao et al., 2003b) but was only present in seven of the samples in the data set. However, a correlation analysis between this species and three other plausible biomass burning tracers revealed excellent correlations (R^2 for NSS potassium = 0.97, for oxalate = 0.96, light absorbing carbon = 0.98) that we utilize in interpreting the source profiles.

Hegg et al. (2008) exercised the EPA receptor model UNMIX 2.3 on the above data set to derive sources. The model found feasible solutions to the matrix inversion only for three factors or sources using the detection algorithm of Henry (2003) that finds data 'edges' in sets of data points in *N*-dimensional space. These sources were interpreted as representing, marine, biomass burning and pollution emissions. The source identification was based primarily on Na and Cl for the marine factor, black carbon and NSS potassium for the biomass and Pb and NSS sulphate for the pollution factor (see Hegg et al. 2008 for details).

Having a plausible source inventory in hand, the next step in the receptor modelling exercise is to quantify the contribution of each source to each of the 24 chemical samples in the database.

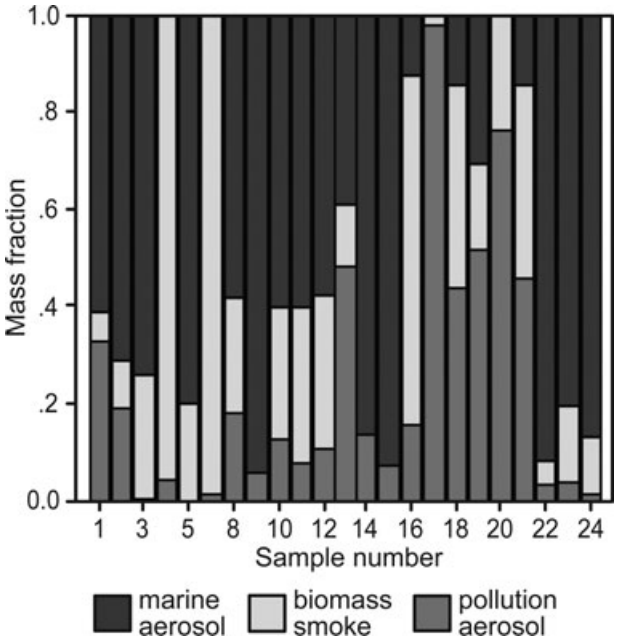

Fig. 1. Mass fractions of each of the three aerosol types in the study area for each of the aerosol samples analysed. From Hegg et al. (2008).

This, of course, is done automatically by the UNMIX model and the model predicted source contributions, reproduced from Hegg et al., are shown in Fig. 1. The contributions are shown as mass fractions of the total aerosol mass present. It can be seen that in about a third of the cases the aerosol is dominated by marine aerosol (i.e. ∼75% of the mass is associated with the marine source). The two cases shown (samples 4 and 6) for which biomass smoke dominated the aerosol are both associated with 4-d back trajectories (HYSPLIT-IV) that passed within a few km of a very large forest fire near Santa Barbara (the second largest in California history). A third sample (16, corresponding to the flight on 24 August) also had a pronounced biomass component and a back trajectory that closed to within ∼100 km of the fire column. Hence, the source attribution is broadly consistent with meteorological data for the fire source. Similarly, pollution aerosol was most evident for samples 13 and 17–21, taken offshore during 25 and 26 August, days during which southerly flow along the coast was present, advecting air from the polluted South Coast Air Basin (the location of metropolitan Los Angeles). A few samples had back trajectories near the fire area (though not as close as those mentioned above) but also were in the broad southerly flow regime. They displayed a more mixed chemical character.

4.2. Overview of the CCN data

CCN activation spectra, as noted above, were measured for 16 of the 24 chemical samples shown in Fig. 1. The directly measured cumulative number concentrations of active CCN at a given supersaturation were regressed onto the standard power formula long used to characterize the activation spectrum, namely: cumulative CCN $= c(\text{supersat})^k$ (cf. Twomey and Squires, 1959). Average values for the fit parameters over the entire data set (see Table 3) were: $c = 772 \pm 20$ cm^{-3} and $k = 0.78 \pm 0.05$. The mean R^2 for the individual spectral fit of any given flight traverse was 0.91 ± 0.1. These values are somewhat higher than expected for background marine air, for which c values on the order of a few hundred, and k's on the order of 0.5 are more typical (*cf.* Hegg and Hobbs, 1992), though there is substantial variance even under background conditions. For the general region off the central California coast, Hudson et al. (2000) measured background c and k values of ∼450 cm^{-3} and 0.65, respectively, in June; Hudson (2007) reported values of c as high as 10^3 cm^{-3} in late July; and Roberts et al. (2006) reported values of c and k, measured in April, of 168 cm^{-3} and 0.4, respectively. While our values are broadly consistent with these data, the values of c and k found here do suggest that the area was impacted by aerosol sources other than the sea surface on a regular basis during the CARMA study. That the area in fact is regularly impacted by a number of different aerosol sources was demonstrated by the analysis of aerosol size spectra presented by Roberts et al. (2006). More tellingly still from the standpoint of this analysis, the receptor modelling results of Hegg et al. (2008) for the CARMA study period examined here suggest that the aerosol in the study area is a mix of particles from three distinct sources, marine, biomass burning and pollution. It is therefore scarcely surprising that the CCN spectral characteristics reflect this mixed origin of the particles. To quantitatively evaluate the contribution of these sources to the overall CCN spectrum, we apply the receptor modelling methods and results of Hegg et al. (2008) to the CCN concentrations.

Table 3. CCN spectral fit parameters for the three different source types found by the receptor model

Source type	c	k	R^2
Marine	328 ± 10	0.72 ± 0.06	0.99
Pollution	234 ± 18	1.2 ± 0.02	0.95
Biomass burning	89 ± 3.9	0.46 ± 0.08	0.95
Total CCN[a]	772 ± 20	0.78 ± 0.05	0.91

[a]Based on the direct CCN measurements, as per Section 4.2.

4.3. Source apportionment of CCN

The methodology for partitioning of a variable into the various source components is well established. To arrive at the contribution of each source to the CCN concentration in each sample, linear regressions of the CCN concentration in each sample onto the normalized factor source contribution for each factor in each

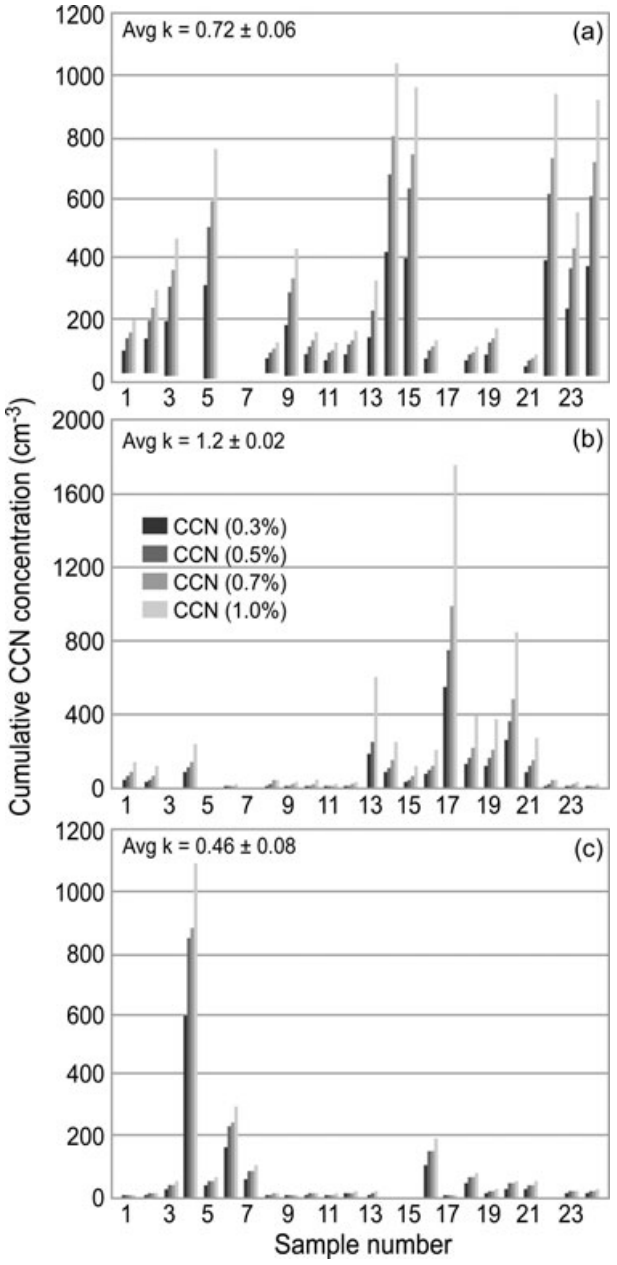

Fig. 2. CCN spectra for each of the samples. Panel (a) is for the marine component, panel (b) for the pollution and panel (c) for the biomass smoke.

sample (as shown in Fig. 1) are made. The linear regression coefficients are then multiplied by the normalized source contributions to arrive at the contribution of each source to the measured CCN concentration in each sample. In this instance, since in fact there are five cumulative CCN concentrations available for each sample, one at each of five supersaturations, five such regressions would normally be done. However, the 0.2 and 0.3 supersaturations are quite close and there is generally little systematic difference between concentrations for these two settings (and the 0.2% data have much larger uncertainties). We therefore performed the regressions only for the four higher supersaturations. Results of this analysis are shown in Fig. 2. In panel (a), the CCN spectra attributable to the marine source are given for each of the samples for which they could be calculated. Similarly, the spectra for the pollution aerosol are given in panel (b) and for the biomass burning aerosol in panel (c). While each source type shows considerable variation in the total CCN concentration (cumulative number activated at 1% supersaturation), the spectral slope (i.e. the k values) seem to be fairly consistent within the source types. To show this more clearly, the average concentrations at the given supersaturations for each of the source categories were fit to the power function formula. Results are given in Table 1 and also shown in Fig. 2. The relatively small standard deviations (and thus the statistically significant differences) of the mean k values for each source support the intra-source homogeneity of the spectral slopes. As expected, the marine power function parameters are more in line with previous results from background marine air (as alluded to above). The pollution CCN spectrum reflects, in its relatively low c value, the secondary contribution of pollution to the overall CCN concentration in our offshore venue. The higher k value is commonplace (though by no means inevitable) in polluted air with large numbers of soluble small particles in the Aitken size range (<80 nm diameter) from secondary production (cf. Seinfeld and Pandis, 1998). The c value for the biomass burning is also consistent with the relatively small contribution of this source to the overall CCN concentration while the low k value is in accord with previous biomass smoke measurements (e.g. Lee et al., 2006; Vestin et al., 2007).

In addition to a partitioning of CCN between sources, it is of interest to see if the partitioning varies with the supersaturation. This might be expected since CCN activity is a function of size (mostly) and composition, and both of these are source dependent (e.g. Roberts et al., 2006; Furutani et al., 2008; Hudson, 2007). However, since the CCN concentrations as given above are cumulative concentrations active at or above a given supersaturation, the differential concentration for a given supersaturation range must first be determined to truly assess the impact of different size distributions and size-dependent composition on the CCN activity. Hence, CCN number concentrations active between 0.3 and 0.5%, 0.5 and 0.7%, and 0.7 and 1.0% supersaturation (equivalent size ranges assuming completely soluble particles: 70–49, 49–38 and 38–30 nm diameter) have been calculated and these values regressed onto the normalized factor source contributions as were the original cumulative concentrations. The mean fractional contribution of each source to the CCN concentration as a function of the supersaturation range is derived from this analysis and presented in Fig. 3. While not an overwhelming trend, it is clear, in particular, that the contribution of the pollution source increases with increasing supersaturation while that of the marine source decreases.

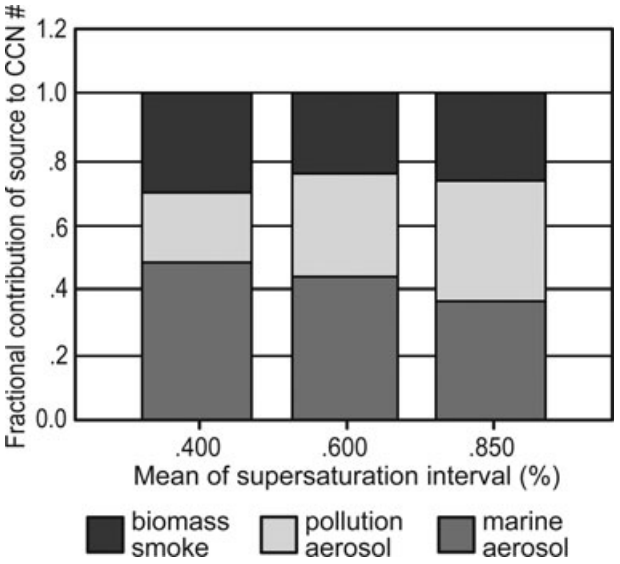

Fig. 3. The fractional contribution of the three sources to the CCN concentration as a function of the supersaturation range.

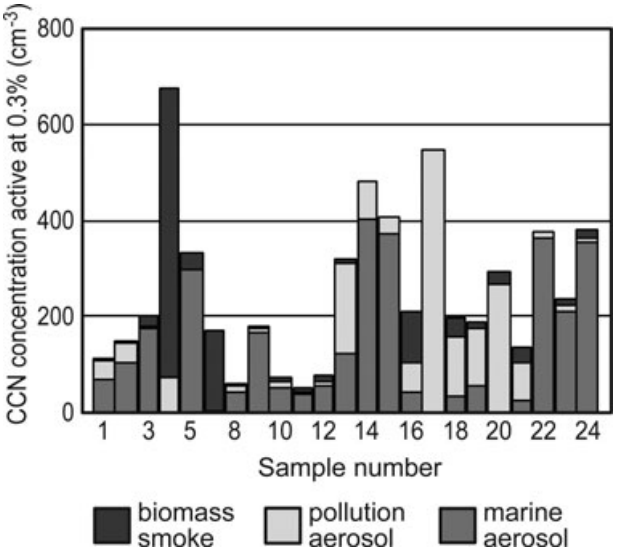

Fig. 4. Source contributions of each of the three sources to each sample taken during the study.

Finally, the paramount question of what fraction of the CCN upon which clouds form come from each of the three sources impacting the CARMA operations area is assessed. This can be done most easily by first addressing the issue of what the effective supersaturation in the clouds in the operation area is, thus controlling for the supersaturation dependence shown in Fig. 3. A long established methodology to estimate cloud supersaturations, that are very difficult to measure directly, is to compare the below cloud CCN activation spectrum with the Cloud Drop Number Concentration (CDNC) in the overlying cloud (e.g. Hudson and Li, 1995). For this comparison, we restricted ourselves to in cloud segments with liquid water content $\geq$90% of the adiabatic value and with drizzle concentrations $\leq$2 cm^{-3} as per Brenguier et al. (2000) in order to minimize the impact of collision-coalescence on the cloud drop number concentration. This yields what is sometimes called the effective supersaturation since it infers the supersaturation from the number of CCN necessary to produce the observed CDNC. The CARMA database yielded 11 cases for which the CCN measurements were sufficiently close to cloud base, and the clouds in which the CDNC were measured were sufficiently close to adiabatic to permit the requisite comparison. The comparison suggests that the clouds had achieved supersaturations in the range from 0.2 to 0.3%. This is in the range long held to be characteristic for marine stratus (cf. Mason, 1971), similar to values found elsewhere for marine stratus (e.g. Hudson and Li, 1995) and in fact essentially the same as that found in earlier studies for stratus in this area in spring (Roberts et al., 2006). Hence, we use the CCN concentration at 0.3% supersaturation in our source analysis for the entire data set. The partitioning of the CCN active at 0.3% supersaturation for each of the samples is shown in Fig. 4. As expected, the marine source is largest but there is substantial variation between samples. CCN samples 4 and 6 are dominated by biomass burning aerosol as was the mass, while pollution is the most prominent source in samples 13 and 17–21, associated with the transport of pollution from the South coast Air Basin. Averaged over all of the samples, the marine source contributes 51% of the CCN number concentration, the pollution 30% and the biomass burning 19%. It is important to note that these percentages differ from the mass partitioning to the various sources, as given in Fig. 1. The mean values for mass are: 51, 22 and 27% for marine, pollution and biomass, respectively. This illustrates the disproportionation between particle number concentration and total mass even at the relatively low supersaturation of 0.3% (corresponding to the relatively large particle activation diameter of $\sim$70 nm). This is especially evident in the pollution case where changes in the smaller, Aitken range, particle concentrations—which correspond to most CCN—have little impact on the total particle mass or, commonly, its composition.

5. Conclusions

The essentially exploratory analysis presented suggests that receptor modelling may be a viable alternative technique to quantifying the contribution of anthropogenic sources to the CCN that impact climate critical cloud systems such as the stratocumulus off the California coast. Biomass burning in the continental region adjacent to the CARMA operational area (offshore, marine cloud-topped boundary layer) is largely human-induced (either accidentally or through prescribed burns). Hence, the anthropogenic component of the CCN in this area might plausibly be considered to have been $\sim$50% during this study. On the other hand, the substantial variability in sources from sample to

sample is in accord with the assertion of Hudson (2007) concerning the variability in CCN activity in marine environments and suggests that other allocations might be expected for different years and even seasons. For example, during a year or season with less biomass burning influence in the area, marine sources could be proportionally larger. Receptor modelling provides a straightforward way of explaining this variability.

6. Acknowledgments

This research was supported by ONR grant N00014–07-1–0277. The authors wish to thank Prof. Tim Larson for many valuable discussions. Back trajectories used in this study were calculated with HYSPLIT-IV (HYbrid Single-Particle Lagrangian Integrated Trajectory) Model, 1997. Web address: http://www.arl.noaa.gov/ready/hysplit4.html, NOAA Air Resources Laboratory, Silver Spring, MD.

References

Avey, L., Garrett, T. J. and Stohl. 2007. A. Evaluation of the aerosol indirect effect using satellite, tracer transport model, and aircraft data from the International Consortium for Atmospheric Research on Transport and Transformation. *J. Geophys. Res.* **112**, doi:10.1029/2006JD007581.

Bond, T. C. and Bergstrom, R. W. 2006. Light absorption by carbonaceous particles: an investigative review. *Aerosol. Sci. Technol.* **40**, 1–41.

Brenguier, J.-L., Pawlowska, H., Schuller, L., Preusker, R., Fischer, J. and co-authors. 2000. Radiative properties of boundary layer clouds: drop effective radius versus number concentration. *J. Atmos. Sci.* **57**, 803–821.

Chen, L.-W. A., Watson, J. G., Chow, J. C. and Magliano, K. L. 2007. Quantifying $PM_{2.5}$ source contributions for the San Joaquin Valley with multivariate receptor models. *Environ. Sci. Technol.* **41**, 2818–2826.

Cheng, M. D., Hopke, P. K., Barrie, L., Rippe, A., Olson, M. and co-authors. 1993. Qualitative determination of source regions of aerosol in Canadian high Arctic. *Environ. Sci. Technol.* **27**, 2063–2071.

Durkee, P. A., Noone, K. J., Ferek, R. J., Johnson, D. W., Taylor, J. P. and co-authors. 2000. The impact of ship-produced aerosols on the microstructure and albedo of warm marine stratocumulus clouds. A test of the MAST hypothesis Li and Lii. *J. Atmos. Sci.* **57**, 2554–2569.

Furutani, H., Dall'osto, M., Roberts, G. and Prather, K. A. 2008. Assessment of the relative importance of atmospheric aging on CCN activity derived from field measurements. *Atmos. Environ.* **42**, 3130–3142.

Gao, S., Hegg, D. A., Covert, D. S. and Jonsson, H. 2003a. Aerosol chemistry, and light-scattering and hygroscopicity budgets during ACE-Asia. *J. Geophys. Res.* **46**, 55–88.

Gao, S., Hegg, D. A., Hobbs, P. V., Kirchstetter, T. W., Magi, B. I. and co-authors. 2003b. Water-soluble organic compounds in aerosols associated with svanna fires in southern Africa: identification, evolution and distribution. *J. Geophys. Res.* **108**, doi:10.1029/2002JD002324.

Gasso, S., Hegg, D. A., Covert, D. S., Collins, D., Noone, K. J. and co-authors. 2000. Influence of humidity on the aerosol scattering coefficient and its effect on the upwelling radiance during ACE-2. *Tellus* **52B**, 546–567.

Hegg, D. A. and Hobbs, P. V. 1992. Cloud condensation nuclei in the marine atmosphere: a review. In: *Proceedings of the Thirteenth International Conference on Nucleation and Atmospheric Aerosols*. Deepak Publishing, Hampton, VA, 181–192.

Hegg, D. A., Covert, D. S., Jonsson, H. and Covert, P. A. 2005. Determination of the transmission efficiency of an aircraft aerosol inlet. *Aerosol Sci. Technol.* **39**, 966–971.

Hegg, D. A., Covert, D. S. and Jonsson, H. H. 2008. Measurements of size-resolved hygroscopicity in the California coastal zone. *Atmos. Chem. Phys.* **8**, 7193–7203.

Henry, R. C. 2003. Multivariate receptor modeling by N-dimensional edge detection. *Chemometrics Intel. Lab. Sys.* **65**, 179–189.

Hudson, J. G. 2007. Variability of the relationship between particle size and cloud-nucleating ability. *Geophys. Res. Lett.* **34**, doi:10.1029/2006GL028850.

Hudson, J. G. and Li, H. 1995. Microphysical contrasts in Atlantic stratus. *J. Atmos. Sci.* **52**, 3031–3040.

Hudson, J. G., Garrett, T. J., Hobbs, P. V., Strader, S. R., Xie, Y. and co-authors. 2000. Cloud condensation nuclei in ship tracks. *J. Atmos. Sci.* **57**, 2696–2706.

IPCC, Climate Change. 2001. *The Scientific Basis: Contributions of Working Group I to the Third Assessment Report of the IPCC* (eds J. T. Houghton and co-editors). Cambridge University Press, New York, 881pp.

Ishizaka, Y. and Adhikari, M. 2003. Composition of cloud condensation nuclei. *J. Geophys. Res.* **108**, doi:10.1029/2002JD002085.

Kim, E., Hopke, P. K., Larson, T. V. and Covert, D. S. 2004. Analysis of ambient particle size distributions using unmix and positive matrix factorization. *Environ. Sci. Technol.* **38**, 202–209.

Lee, Y. S., Collins, D. R., Runjun, L., Bowman, K. P. and Feingold, G. 2006. Expected impact of an aged biomass burning aerosol on cloud condensation nuclei and cloud droplet concentrations. *J. Geophys. Res.* **111**, doi:10.1029/2005JD006464.

Mason, B. J. 1971. *The Physics of Clouds* 2nd Edition. Clarendon Press, Oxford, 671.

Murphy, D. M., Cziczo, D. J., Froyd, K. D., Hudson, P. K., Mathew, B. M. and co-authors. 2006. Single-particle mass spectroscopy of tropospheric aerosol particles. *J. Geophys. Res.* **111**, doi:10.1029/2006JD007340.

Novakov, T. and Penner, J. E. 1993. Large contribution of organic aerosols to cloud-condensation-nuclei concentrations. *Nature* **365**, 823–826.

Phinney, L., Leaitch, W. R., Lohmann, U., Boudries, H., Worsnop, D. R. and co-authors. 2006. Characterization of aerosol over the sub-arctic east Pacific Ocean. *Deep-Sea Res., Part II* **53**, 2410–2433.

Platnick, S. and Twomey, S. 1994. Determining the susceptibility of cloud albedo to changes in droplet concentration with the Advanced Very High Resolution Radiometer. *J. Appl. Meteorol.* **33**, 334–347.

Platnick, S., Durkee, P. A., Nielsen, K., Taylor, J. P., Tsay, S.-C. and co-authors. 2000. The role of background cloud microphysics in the radiative formation of ship tracks. *J. Atmos. Sci.* **57**, 2607–2724.

Rivera-Carpio, C. A., Corrigan, C. E., Novakov, T., Penner, J. E., Rogers, C. F. and co-authors. 1996. Derivation of contributions of sulfate and carbonaceous aerosols to cloud condensation nuclei from mass size distributions. *J. Geophys. Res.* **101**, 19483–19493.

Roberts, G. and Nenes, A. 2005. A continuous-flow streamwise thermal-gradient CCN chamber for airborne measurements. *Aerosol Sci. Technol.* **39**, 206–221.

Roberts, G., Mauger, G., Hadley, O and Ramanathan, V. 2006. North American and Asian aerosols over the eastern Pacific Ocean and their role in regulating cloud condensation nuclei. *J. Geophys. Res.* **111**, doi:10.1029/2005JD006661.

Schmid, B., Hegg, D. A., Wang, J., Bates, D., Redemann, J. and co-authors. 2003. Column closure studies of the lower tropospheric aerosol and water vapor during ACEAsia using airborne sunphotometer, airborne in-situ and ship-based lidar measurements. *J. Geophys. Res.* **108**, 8656, doi:10.1029/2002JD003361.

Seinfeld, J. H. and Pandis, S. N. 1998. *Atmospheric Chemistry and Physics*. Wiley-Interscience, New York, 1326.

Simoneit, B. R.T., Schaur, J. J., Nolte, C. G., Oros, D. R., Elias, V. O. and co-authors. 1999. Levoglucsan: a tracer for cellulose in biomass burning and atmospheric particles. *Atmos. Environ.* **33**, 173–182.

Song, X.-H., Hopke, P. K., Fergenson, D. P. and Prather, K. A. 1999. Classification of single particles analyzed by ATOFMS using an artifical neural network, ART-2A. *Anal. Chem.* **71**, 860–865.

Twomey, S. and Squires, P. 1959. The influence of cloud nucleus population on the microstructure and stability of convective clouds. *Tellus* **11**, 408–411.

Vestin, A., Rissler, J., Swietlicki, E., Frank, G. P. and Andreae, M. O. 2007. Cloud-nucleating properties of the Amazonian biomass burning aerosol: cloud condensation nuclei measurements and modeling. *J. Geophys. Res.* **112**, doi:10.1029/2006JD008104.

Virkkula, A., Ahlquist, N. N., Covert, D. S., Arnott, W. P., Sheridan, P. J. and co-authors. 2005. Modification, calibration and a field test of an instrument for measuring light absorption by particles. *Aerosol Sci Technol.* **39**, 68–83.

Wang, J., Flagan, R. C., Seinfeld, J. H., Jonsson, H. H., Collins, D. R. and co-authors. 2002. Clear-column radiative closure during ACE-Asia: comparison of multiwavelength extinction derived from particle size and composition with results from sunphotometry. *J. Geophys. Res.* **107**(D23), 4688, doi:10.1029/2002JD002465.

Warren, S. G., Hahn, C. J., London, J., Chervin, R. M. and Jenne, R. L. 1988. Global Distribution of Total Cloud Cover and Cloud type Amounts Over the Ocean. NCAR Technical Note NCAR/TN-317+STR.

Willis, R. D., Ellenson, W. D. and Conner, T. L. 2001. Monitoring and source apportionment of particulate matter near a large phosphorous production facility. *J. Air Waste Manage. Assoc.* **51**, 1142–1166.